Accepted to ApJ Letters
Preprint typeset using LaTeX style emulateapj

arXiv:astro-ph/0101465v1 25 Jan 2001

CO DETECTIONS OF EDGE-ON LOW SURFACE BRIGHTNESS GALAXIES

L. D. Matthews[1]
Yu Gao[2]

Accepted to ApJ Letters

ABSTRACT

We have obtained deep CO(1-0) observations of 8 nearby, edge-on, low surface brightness (LSB) spiral galaxies using the NRAO 12-m telescope. We report detections of 3 of our targets at $> 4\sigma$ level as well as one marginal ($\sim 3\sigma$) detection. These are among the first direct detections of molecular gas in late-type, LSB spirals. Using a Galactic CO-to-H$_2$ conversion factor, we derive $M_{H2} \sim 1.4 - 3.5 \times 10^7\ \mathcal{M}_\odot$ and M_{H2}/M_{HI}~0.010-0.055 for the detected sources, with 3σ upper limits of $M_{H2} \lesssim 0.7 - 5.7 \times 10^7\ \mathcal{M}_\odot$ and $M_{H2}/M_{HI} \lesssim$0.006-0.029 for the undetected objects.

Subject headings: galaxies: general—galaxies: ISM—galaxies: spiral—ISM: molecules

1. INTRODUCTION

Low surface brightness (LSB) disk galaxies can be defined as rotationally-dominated galaxies with extrapolated central surface brightnesses $\mu_B(0) \gtrsim$23 mag arcsec^{-2}. Numerous studies have now shown that these are not abnormal objects, but rather are a common product of disk galaxy formation and evolution.

Compared with disk galaxies of high surface brightness (HSB), most late-type LSBs tend to be H I-rich, with diffuse, low-density stellar disks, and metallicities $\lesssim$1/3 solar (e.g., McGaugh 1994). This suggests that LSB galaxies have been inefficient star-formers over their lifetimes. Indeed, H I surface densities in LSB galaxies are often observed to be well below the critical threshold for star formation (e.g., van der Hulst et al. 1993). Nonetheless, LSB galaxies typically contain some signatures of ongoing star formation, including modest amounts of Hα emission (e.g., Schombert et al. 1992) and blue colors indicative of young stellar populations (e.g., McGaugh & Bothun 1994; Matthews & Gallagher 1997).

In spite of the evidence for modest ongoing star formation, a number of observational and theoretical arguments suggest that LSB galaxies may be extremely molecular gas-deficient systems. For example, LSB galaxies are generally found to be dust-poor (e.g., Matthews & Wood 2001; hereafter MW01). This, combined with possible low interstellar pressures, and the lack of the cooling effects of metals, might be expected to impede molecular gas formation (e.g., Gerritsen & de Blok 1999; Mihos, Spaans, & McGaugh 1999). Nonetheless, MW01 have shown that the edge-on LSB galaxy UGC 7321 contains a clumpy ISM structure, including candidates for dark clouds, indicating that it may have both the conditions and the catalysts for the formation of H$_2$ and other molecules.

Despite this circumstantial evidence for molecular gas, several groups have tried and failed to detect CO emission from late-type LSB galaxies (Schombert et al. 1990; Knezek 1993; de Blok & van der Hulst 1998). However, these observations used only modest integration times, and are sufficient only to put upper limits on their molecular gas contents of M_{H2}/M_{HI} $\leq$0.07-0.43. In fact, many of these values are consistent with the M_{H2}/M_{HI} ratios typical of HSB Sd-Sm galaxies (Young & Knezek 1989) and therefore tell us little about how the molecular gas contents of LSB spirals may differ. Recently, O'Neil, Hofner, & Schinnerer (2000) reported deeper CO observations of 4 red LSBs, including a detection of one object. However, the large H I linewidth of the detected galaxy (W_{20} = 430 km s^{-1}) suggests it is one of the class of relatively rare LSB giants (e.g., Sprayberry et al. 1995; Matthews, van Driel, & Monnier-Ragaigne 2001) and may be somewhat different in nature from typical late-type LSBs. Motivated by these factors, we have undertaken new deep CO(1-0) observations of 8 late-type, low-mass, LSB spirals.

2. SAMPLE SELECTION

For our survey we selected a sample of bulgeless, edge-on LSB galaxies of types Scd-Sm. Targets of relatively large angular size ($>2.\!'5$) were chosen so that the telescope beam would be well matched to the expected CO-emitting regions in the inner disk. We present here results for 8 galaxies with integration times $t \gtrsim$5.5 hours. Some general properties of our targets are summarized in Table 1.

Although the *observed* surface brightnesses of our edge-on sample are enhanced due to projection, their LSB natures are evident from optical imaging and surface photometry (see Table 1). All have a diffuse, transparent appearance, lack a true dust lane, and have relatively high M_{HI}/L_B ratios. In addition, all of these objects have low star formation rates as evidenced by their weak or undetectable 1.4GHz radio continuum fluxes in the NVSS survey (Condon et al. 1998).

We chose to emphasize edge-on LSB galaxies in the present study since projected gas surface densities are increased for edge-on viewing angles, hence the detectability of CO is maximized. In addition, edge-on systems provide

---

[1] National Radio Astronomy Observatory, 520 Edgemont Road, Charlottesville, VA 22903 USA, Electronic mail: lmatthew@nrao.edu

[2] Infrared Processing and Analysis Center, MS 100-22, Caltech, Pasadena, CA 91125

us with a greatly enhanced ability to identify dark cloud candidates and obtain complementary measurements of the structure of the dust and ionized gas (e.g., MW01).

3. DATA ACQUISITION AND REDUCTION

Our data were obtained with the NRAO[3] 12-m Telescope at Kitt Peak. Most observations were done in 1999 June, with some additional data acquired in 1997 January and 1999 December. At 115.2GHz, the 12-m telescope has a beam of FWHP$\sim 55''$. Typical system temperatures during our runs were $T_R^* \sim$270–400K.

Our observations employed the 3mm dual SIS receivers and the two 256×2MHz filter bank spectrometers. Telescope pointing and focus were checked frequently by observing planets or bright quasars. Data were obtained in BSP (beam+position switching) mode using the nutating secondary with a beam throw $\pm 2'$–$3'$. To eliminate spurious signals, we obtained roughly half of our data with the source velocity offset ± 50 km s^{-1} from the bandpass center. For all 8 targets we obtained data at the optical center of the galaxy. We also observed some offsets along the major axes of UGC 7321 and NGC 4244 (Table 2).

Our data were calibrated by performing a vane (chopper wheel) measurement after every other 6-minute scan. Our absolute calibration was also checked by measuring the CO line strength of M82 at least once during each observing run. We estimate an absolute flux accuracy of ∼20%.

We reduced our spectra using the CLASS and Unipops analysis packages. All scans were individually inspected, and those with highly structured baselines were discarded. Scans were also examined in blocks according to acquisition time in order to check for recurrent spurious signals. Channels repeatedly exhibiting positive or negative spikes $> 3\sigma$ above the rms noise were blanked and substituted with values interpolated from the adjacent channels. Next a velocity window was chosen from H I data, and a linear baseline was subtracted from each scan. All remaining scans were then assigned weights according to their mean rms noise and averaged to obtain the final spectra.

4. RESULTS

The final spectra for each of our target galaxies are shown in Figure 1. The data are smoothed to a resolution of ∼20–40 km s^{-1} to enhance signal-to-noise. We detect the CO(1-0) line at $> 4\sigma$ (after smoothing) in 3 of our targets (UGC 2082, UGC 7321, NGC 4244), and marginally detect one object (UGC 6667) at $\sim 3\sigma$. These represent some of the first direct detections of molecular gas in late-type, LSB spiral galaxies. Table 2 summarizes CO linewidths at 50% peak maximum ($W_{50,CO}$), line centroids (V_{CO}), and integrated CO line intensity ($I_{\rm CO} = \int T_R^* dV$), measured for the detected galaxies using Gaussian fits.

To within observational uncertainties we find that the line centroids of our detected signals show good agreement with H I systemic velocities of these galaxies from the literature (see Table 1). In addition, the CO linewidths of our putative detections are roughly comparable with the H I linewidths. This would be expected for CO spread over the central few kpc of these LSB galaxies, as is generally found in late-type spirals (e.g., Young & Knezek 1989).

One of our detected sources (NGC 4244) was previously detected in CO by Sage (1993a,b), offering corroborating evidence that our detection is real. Like Sage (1993a,b) we detected CO(1-0) emission both at the optical center of the galaxy as well as at offset positions along the major axis. However, the strengths of our measured lines are much weaker. Since we used significantly longer integrations and the 12-m system performance is much improved since the late 1980's, our new data strongly suggest that NGC 4244 is a weaker CO source than previously reported.

For the 4 galaxies where no clear signal was detected, we compute 3σ upper limits using:

$$I_{CO} \leq 3T_{rms} \cdot W_{20,HI}/[f \times (1 - W_{20,HI}/W)]^{0.5} \qquad (1)$$

where T_{rms} is the rms noise in the final spectrum in mK, $W_{20,HI}$ is the H I linewidth, $f = W_{20,HI}/\delta_c$, δ_c is the channel spacing in km s^{-1} and W is the entire velocity coverage of the spectrum (Gao 1996). These upper limits are summarized in Table 3.

5. DISCUSSION

We estimate the total mass of molecular hydrogen within the $55''$ telescope beam (Table 3) from:

$$M_{H2} = 4.78[(\pi/(4\ln 2)I_{CO}d_b^2]\epsilon^{-1} \quad (M_\odot) \qquad (2)$$

where I_{CO} is the integrated CO line flux in K·km s^{-1} (T_R^* scale), d_b^2 is the telescope beam diameter in pc at the distance of the galaxy, and ϵ is the main beam efficiency of the telescope (0.84 at 115.3 GHz for the 12-m as of 2000 January). This formula assumes a Gaussian beam and a standard Galactic value of the CO-to-H$_2$ conversion factor $X = N(H_2)/\int T(CO)dV = 3.0 \times 10^{20}$cm^{-2}/[K km s^{-1}] (where $T(CO) = T_R^*/\epsilon$; e.g., Young & Scoville 1991), which is applicable to the molecular clouds at virial equilibrium. For galaxies where data were obtained at off-center pointings, the total H$_2$ mass was estimated by summing the individual spectra according to Eq. 3 of Sage (1993a).

The applicability of the standard X factor to the diffuse, low metallicity environments of LSB galaxies remains highly controversial (e.g., Maloney & Black 1988; Mihos et al. 1999), as low densities, low metallicities, and low dust contents in LSBs would all seemingly argue in favor a higher X value, while clumpiness of the ISM and/or the absence of a strong UV dissociating flux may somewhat lower this number. This creates some uncertainty in our M_{H2} estimates. Moreover, our derived CO fluxes should be regarded as conservative, since data were obtained at offset pointings only for NGC 4244 and UGC 7321, and since some shadowing may occur in edge-on galaxies if the CO is optically thick. However, this latter effect is expected to be small for LSB systems, and based on the typical sizes of CO-emitting regions in late-type galaxies, it is unlikely in the present survey that a significant fraction of CO-emitting gas lay outside our beam (see also below).

Previous null detections of CO in LSB galaxies have been interpreted to suggest that either CO does not trace H$_2$ in these galaxies or simply that LSB galaxies are devoid of molecular gas. It has even been postulated that stars may form directly from atomic hydrogen in these galaxies (e.g., Schombert et al. 1990). Our new observations show that at least some low-mass, late-type LSB galaxies do contain a modest molecular gas component. If the Galactic X factor is adopted, we find the implied M_{H2}/M_{HI} ratios (0.010-0.055; Table 3) are several times smaller than those typically found for brighter Sd-Sm spirals (0.19±0.10) by Young & Knezek (1989). However, this does not seem unexpected for dim, diffuse galaxies that are inefficient at converting their raw, atomic gas into stars.

---

[3] The National Radio Astronomy Observatory (NRAO) is a facility of the National Science Foundation operated under cooperative agreement by Associated Universities, Inc.

The strength of FIR (60 and 100μm) emission is well known to correlate with CO strength in HSB galaxies (e.g., Sage 1993a), and all 3 of our CO-detected LSBs were detected by *IRAS* (Table 1). We find these galaxies follow the FIR-M_{H2} correlation of Sage (1993a), suggesting that their inferred molecular gas supplies are adequate to sustain their observed star formation rates and that we have not grossly (i.e., by more than a factor of a few) underestimated their total H_2 contents.

In our present sample we find no other obvious correlations between detection in CO and global properties (e.g., color, M_{HI}/L_B). This may simply reflect our small sample size, and underscores the need for more molecular gas observations of larger samples of LSB galaxies.

6. SUMMARY

We have presented deep CO(1-0) observations of 8 edge-on, late-type, LSB spiral galaxies. These are among the most sensitive CO observations of LSB galaxies obtained to date. We have detected 3 of our targets galaxies at a $> 4\sigma$ level, and have marginally detected one object at $\sim 3\sigma$. These represent some of the first direct detections of molecular gas in low-mass, late-type LSB spiral galaxies. Adopting a Galactic CO-to-H_2 conversion factor, we find values of $M_{H2} = 1.4 - 3.5 \times 10^7\ \mathcal{M}_\odot$ for the detected galaxies, and upper limits $M_{H2} \lesssim 0.7 - 5.7 \times 10^7\ \mathcal{M}_\odot$ for the undetected objects. LSB spirals appear to be deficient in molecular gas relative to their atomic gas contents compared with brighter spirals of similar Hubble type, although the validity of the Galactic CO-to-H_2 conversion factor for these systems is still controversial.

We thank the observing staff at the 12-m Telescope, as well as W. van Driel and D. Monnier-Ragaigne for their contributions in support of this project. An anonymous referee also provided useful comments. This research made use of the NASA/IPAC Extragalactic Database (NED) which is operated by JPL under contract with NASA.

REFERENCES

Condon, J. J. et al. 1998, AJ, 115, 1693
de Blok, W. J. G. & van der Hulst, J. M. 1998, A&A, 336, 49
Fry, A. M., Morrison, H. L., Harding, P., & Boroson, T. A. 1999, AJ, 118, 1209
Gao, Y. 1996, Ph.D. Thesis, State Univ. of New York at Stony Brook
Gerritsen, J. P. E. & de Blok, W. J. G. 1999, A&A, 342, 655
Helou, G., Khan, I. R., Malek, L., & Boehmer, L. 1988, ApJS, 68, 151
Knezek, P. M. 1993, Ph.D. Thesis, Univ. of Massachusetts
Maloney, P. & Black, J. H. 1988, ApJ, 325, 389
Matthews, L. D. & Gallagher, J. S. 1997, AJ, 114, 1899
Matthews, L. D., Gallagher, J. S., & van Driel, W. 1999, AJ, 118, 2751
Matthews, L. D., Gallagher, J. S., & van Driel, W. 2000, in Galaxy Dynamics: from the Early Universe to the Present, ed. R F. Combes, G. A. Mamon, & V. Charmandaris, (San Francisco: ASP), 195
Matthews, L. D., van Driel, W., & Monnier-Ragaigne, D. 2001, A&A, 365, 1
Matthews, L. D. & Wood, K. 2001, ApJ, 548, in press (MW01)
McGaugh, S. S. 1994, ApJ, 426, 135
McGaugh, S. S. & Bothun, G. D. 1994, AJ, 107, 530
Mihos, J. C., Spaans, M., & McGaugh, S. S. 1999, ApJ, 515, 89
Olling, R. P. 1996, AJ, 112, 457
O'Neil, K., Hofner, P., & Schinnerer, E. 2000, ApJ, 545, L99
Prugniel, P. & Heraudeau, P. 1998, A&AS, 128, 299
Sage, L. J. 1993a, A&A, 272, 123
Sage, L. J. 1993b, A&AS, 100, 537
Sanders, D. B. et al. 1986, ApJ, 305, 45
Schombert, J. M., Bothun, G. D., Impey, C. D., & Mundy, L. G. 1990, AJ, 100, 1523
Schombert, J. M., Bothun, G. D., Schneider, S. E., & McGaugh, S. S. 1992, AJ, 103, 1107
Sprayberry, D., Impey, C. D., Bothun, G. D., & Irwin, M. J. 1995, AJ, 109, 558
Tifft, W. G. & Cocke, W. J. 1988, ApJS, 67, 1
Tully, R. B. 1988, Nearby Galaxies Catalog (Cambridge: Cambridge University Press)
Tully, R. B. Pierce, M. J., Huang, J.-S., Saunders, W., Verheijen, M. A. W., & Witchalls, P. L. 1998, AJ, 115, 2264
van der Hulst, J. M., Skillman, E. D., Smith, T. R., Bothun, G. D., McGaugh, S. S., & Bothun, G. D. 1993, AJ, 106, 548
Verheijen, M. A. W. 1997, Ph.D. Thesis, University of Groningen
Young, J. S. & Knezek, P. M. 1989, ApJ, 347, L55
Young, J. S., & Scoville, N. Z. 1991, ARA&A, 29, 581

TABLE 1
PROPERTIES OF THE TARGET GALAXIES

Name	T	V_h (km s^{-1})	D (Mpc)	i ($^\circ$)	D_{25} ($'$)	logL_B ($L_\odot$)	$B-R$ (mag)	$\mu(0)_{B,i}$ (mag $''^{-2}$)	$\bar{\mu}_{B,i}$ (mag $''^{-2}$)	$W_{20,HI}$ (km s^{-1})	logM_{HI} ($M_\odot$)	L_{FIR} ($10^7 L_\odot$)	Ref.
UGC711	Sd	1982	15.0	89	4.65	8.96	0.87	24.4	25.8	230	9.04	···	2,4,7
UGC2082	Sc	707	10.7	90	5.94	9.10	1.34	···	25.8	214	9.12	10.1	6,8
UGC4148	Sm	737	12.8	90	2.52	8.69	···	···	···	148	8.68	···	8
IC2233	Sd	563	10.0	90	5.17	9.15	0.58	23.1	24.8	206	9.08	7.0	4,8
UGC6667	Scd	979	15.5	90	3.70	9.17	0.96	23.8	···	188	8.80	···	9
NGC4244	Scd	244	3.6	84	19.4	9.36	0.6:	23.6:	24.4	180	9.13	13.4	1,5,6,8
UGC7321	Sd	407	10.0	88	5.54	9.00	0.99	23.6	25.6	233	9.04	7.9	3
UGC9242	Sd	1440	20.6	90	5.66	9.55	0.78	23.7	25.7	205	9.29	···	4,8

NOTE.—Explanation of columns: (1) name; (2) Hubble type; (3) heliocentric H I recessional velocity; (4) distance; (5) inclination; (6) angular diameter; (7) logarithm of B-band luminosity; (8) $B-R$ color; (9) B-band central surface brightness (corrected for inclination and internal extinction); (10) mean B-band disk surface brightness within the outermost observed isophote (corrected for inclination and internal extinction); (11) H I linewidth at 20% peak maximum; (12) logarithm of the H I mass; (13) FIR luminosity [see Helou et al. (1988)]; (14) references for quoted optical and H I parameters. Type, V_h, D_{25}, and *IRAS* 60μm and 100μm fluxes were taken from NED. The B-band central surface brightness of NGC 4244 was estimated using Table 3 of Ref. 1, and its global $B-R$ color was estimated from $B-R \approx 1.5(B-V)+0.10$. If not quoted in the original references, B-band internal extinctions were estimated using Tully et al. (1998) and surface brightnesses were corrected to face-on using Eq. A4 of Ref. 3 assuming $h_r/h_z \approx a/b$.

REFERENCES.—(1) Fry et al. (1999); (2) Gallagher et al., in prep.; (3) Matthews et al. (1999); (4) Matthews, Gallagher, & van Driel (2000); (5) Olling (1996); (6) Prugniel & Heraudeau (1998); (7) Tifft & Cocke (1988); (8) Tully (1988); (9) Verheijen (1997).

TABLE 2
SUMMARY OF OBSERVATIONS

Name	α_{1950} ($^{h\ m\ s}$)	δ_{1950} ($^\circ\ '\ ''$)	t (hours)	T_{rms} (mK)	T_{sys} (K)	δ_c (km s^{-1})	Offset (arcsec)
UGC711[a]	010602	+012229	5.5	0.94	525	41.6	(0,0)
UGC2082	023322	+251222	7.8	0.67	399	41.6	(0,0)
UGC4148	075657	+421953	6.0	1.05	340	20.8	(0,0)
IC2233	081027	+455343	7.8	0.72	317	20.8	(0,0)
UGC6667	113945	+515232	8.9	0.68	354	41.6	(0,0)
NGC4244a	121500	+380509	7.2	1.10	325	20.8	(0,0)
NGC4244b	″	″	1.6	2.37	358	20.8	(−21.9,−20.)
NGC4244c	″	″	5.1	1.15	319	20.8	(+45.,+40.)
NGC4244d	″	″	7.0	1.22	332	20.8	(−46.,−30.)
NGC4244e	″	″	2.0	2.03	316	20.8	(+46.,+30.)
UGC7321a	121503	+224903	15.0	0.47	340	20.8	(0,0)
UGC7321b	″	″	13.4	0.60	308	20.8	(−27.,−3.8)
UGC9242	142319	+394550	5.6	0.98	330	41.6	(0,0)

[a] Receiver 2 exhibited anomalously high T_{sys} during observations of UGC 711.

NOTE.—Explanation of columns: (1) galaxy name; (2) & (3) B1950.0 coordinates (4) total usable integration time; (5) spectrum rms; (6) mean system temperature of all averaged scans; (7) velocity width of channels in final spectrum, after Hanning smoothing; (8) coordinates of observations, in units of arcseconds north and east from the target's optical center.

TABLE 3
MEASURED CO PARAMETERS

Name	V_{CO} (km s^{-1})	$W_{50,CO}$ (km s^{-1})	I_{CO} (K·km s^{-1})	S/N	M_{H2} ($10^7 M_\odot$)	M_{H2}/M_{HI}
UGC711	⋯	⋯	≤0.30	⋯	≤3.14	≤0.028
UGC2082	725.9 (15.0)	176.9 (26.4)	0.57 (0.09)	4.7	2.98	0.022
UGC4148	⋯	⋯	≤0.17	⋯	≤1.24	≤0.026
IC2233	⋯	⋯	≤0.15	⋯	≤0.71	≤0.0058
UGC6667	971.4: (15.0)	161.7: (44.3)	0.32: (0.08)	2.9	3.52	0.055
NGC4244a	217.1 (8.7)	194.4 (24.6)	0.91 (0.08)	6.3	0.54	⋯
NGC4244b	213.4: (31.7)	223.9: (57.2)	0.75: (0.20)	2.9	0.44	⋯
NGC4244c	193.5 (8.1)	126.0 (21.5)	0.85 (0.10)	5.8	0.50	⋯
NGC4244d	249.0 (17.0)	89.6 (41.9)	0.70 (0.22)	4.7	0.42	⋯
NGC4244e	211.2 (5.7)	51.5 (11.6)	0.43 (0.09)	3.8	0.26	⋯
NGC4244(sum)	227.4 (5.9)	136.6 (12.7)	2.32	⋯	1.36	0.010
UGC7321a	385.9 (10.0)	168.2 (25.7)	0.50 (0.06)	8.2	2.30	⋯
UGC7321b	469.5 (8.6)	75.0 (20.1)	0.20 (0.04)	4.5	0.92	⋯
UGC7321(sum)	420.5 (10.9)	190.3 (21.2)	0.71	⋯	3.22	0.029
UGC9242	⋯	⋯	≤0.30	⋯	≤5.75	≤0.029

NOTE.—CO line parameters are measured from Gaussian fits; upper limits are derived as described in Sect. 4. Uncertainties in measured quantities are given in parentheses following the entry. A colon (:) following a table entry indicates a marginal ($\sim 3\sigma$) detection. Explanation of columns: (1) name; (2) velocity centroid of CO(1-0) line; (3) full width at 50% peak maximum of the CO(1-0) line; (4) integrated CO(1-0) line flux (T_R^* scale) derived from a Gaussian fit; upper limits are given for cases where no signal was detected at $\gtrsim 3\sigma$; fluxes may be converted to Jy by multiplying by the conversion factor $f_1 \approx$35 Jy/K; (5) signal-to-noise of the detected CO line; (6) estimate of the mass of molecular hydrogen within the 55″ FWHP beam (see Sect. 5); (7) ratio of the estimated amount of molecular hydrogen to the total H I mass of the galaxy. Entries denoted "sum" are derived by summing observations at multiple pointings (see Sect. 5.)

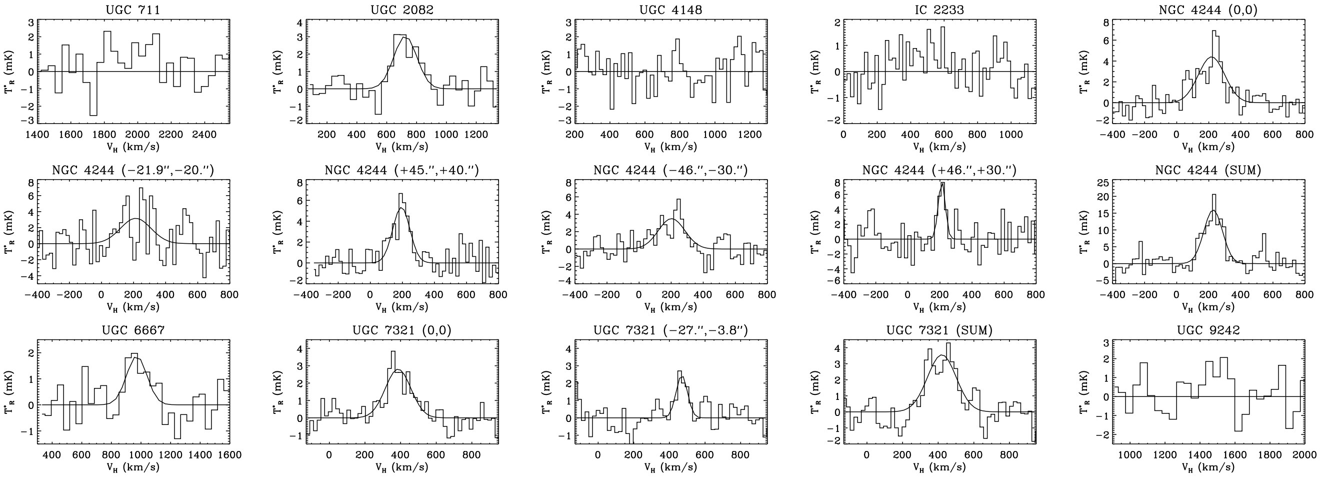

FIG. 1.— CO(1-0) spectra of 8 edge-on, late-type, low surface brightness galaxies obtained with the NRAO 12-m telescope. Axes are radial velocity (in km s^{-1}) versus CO antenna brightness temperature in mK (T_R^* scale). Overplotted lines show Gaussian fits if a signal was detected. The spectra marked 'SUM' show the combined results of multiple pointing observations.